JOURNAL OF Materials CHEMISTRY

Morphology of electrodeposited WO_3 studied by atomic force microscopy

Peikang Shen, Ning Chi and Kwong-Yu Chan*

Department of Chemistry, The University of Hong Kong, Pokfulam Road, Hong Kong, SAR of China

Received 19th October 1999, Accepted 7th January 2000

Electrochromic WO_3 was prepared on highly oriented pyrolytic graphite (HOPG) by electrodeposition under constant current in an alcohol-containing solution. The morphology and the early stage growth mechanism of electrodeposited WO_3 were studied by tapping mode atomic force microscopy (TMAFM). The series of AFM images showed how the morphology of WO_3 formed on HOPG was affected by the electrodeposition parameters. WO_3 electrodeposited on HOPG has a porous structure and exhibits a self-leveling process. The effects of current density, current efficiency, and hydrogen evolution on the morphology were discussed.

Since Deb's electrochromic experiments on solid tungsten trioxide (WO_3) in 1969,[1] significant progress has been made in fundamental and practical investigations which have been well summarized in a recent book[2] and reviews.[3,4] Electrochromic WO_3 can be prepared by different methods. Electrodeposited WO_3 exhibits a very fast response time and good write–erase efficiency.[5,6] The electrochromic properties of WO_3 depend strongly on its morphology and structure. Investigations on the microscopic structural and surface properties of WO_3 have been developed using advanced modern techniques like scanning tunneling microscopy (STM)[7] and atomic force microscopy (AFM).[8] However, there is still a lack of microscopic information about the electrodeposition of WO_3. The deposition mechanism and the effect of the preparative conditions on the WO_3 properties will be better understood based on the microscopic information.

On the other hand, WO_3 codeposited with platinum showed high catalytic activity for the electro-oxidation of small organic molecules like methanol, formic acid and formaldehyde.[9,10] The oxidation of small organic molecules proceeds by a dehydrogenation process. Use of a Pt/WO_3 catalyst can speed up this process since hydrogen adsorbed on the Pt surface can be spilled over to WO_3 and be discharged there. Pt/WO_3 also showed the additional function of tolerance to CO poisoning. However, it was predicted that the highest catalytic activity will be achieved with mixing of Pt and WO_3 at the atomic level. This will depend on the optimisation of preparation conditions and characterisation using new techniques. Atomic force microscopy is able to observe the distribution and morphology of codeposited catalysts.

In this paper, we use tapping mode atomic force microscopy (TMAFM) to observe the growth process and the microstructure of WO_3 on HOPG during electrodeposition. The TMAFM images are obtained under different deposition conditions. A growth mechanism for WO_3 at early stages of the deposition process is proposed.

Experimental

Highly oriented pyrolytic graphite (HOPG) was used as the substrate since its surface is stable, atomically smooth, and has relatively weak interactions with nano-scale deposits. A three-electrode PTFE cell with a Pt counter electrode and an Ag/AgCl reference electrode was used for both electrochemical deposition and measurements. The circular area of the graphite surface exposed to the solution was restricted to 0.28 cm^2 by an O-ring.

Solutions were prepared from A.R. quality chemicals and Milli-Q water (18.2 MΩ cm). The HOPG electrode was freshly exfoliated for each test. Tungsten in powder form was predissolved in 30% hydrogen peroxide aqueous solution. After complete dissolution of the tungsten, a platinum black foil was dipped into the solution to decompose the excess hydrogen peroxide. The plating solution was then prepared, consisting of 10 mmol dm^{-3} dissolved tungsten solution, 0.1 mol dm^{-3} H_2SO_4 and 30% ethanol. Tungsten trioxide was then cathodically deposited under a constant current at room temperature ($\approx$22 °C). The electrode was gently washed with Milli-Q water after each run. The details of the preparation of the tungsten solution and of the WO_3 deposition have been described previously.[5,11] The use of an alcohol-containing solution can stabilize the solution and extend the storage time. On the other hand, previous work has shown that WO_3 prepared in such a solution is more porous which greatly increases the coloration efficiency. In this paper, we examine the effect of the solution composition on the microstructure of the deposited WO_3. The electrochemical characterization was carried out in 0.1 mol dm^{-3} H_2SO_4 solution. Normally, the same piece of graphite was used to maintain reproducibility. All chemicals were supplied and used as received.

Electrochemical measurements were carried out on an EG&G PAR 263 Potentiostat/Galvanostat controlled by 270 Research Electrochemistry Software. The tapping mode atomic force microscopy (TMAFM) images were obtained using a Digital Instruments nanoscope-IIIA in air at room temperature. The AFM tip is n-type silicon (the tip half angle is 17° on each side, 0° on the front, 35° on the back, and the radius of curvature is less than 10 nm) mounted on a cantilever 4.1 ± 0.2 μm thick, 32 μm wide and 121 μm long with a force constant of 51 N m^{-1} (Fluoroware Inc., Germany). The mean resonance frequency is 358 kHz. All images were recorded in 256×256 pixels.

Results and discussion

Fig. 1 shows a typical cyclic voltammogram of WO_3 deposited on a HOPG surface at a cathodic current of 10 μA for 100 s. The plot shows well-defined reduction–oxidation peaks, which correspond to the reversible coloration–bleaching of WO_3.[6] The cyclic voltammogram of HOPG is shown in Fig. 1(b) for

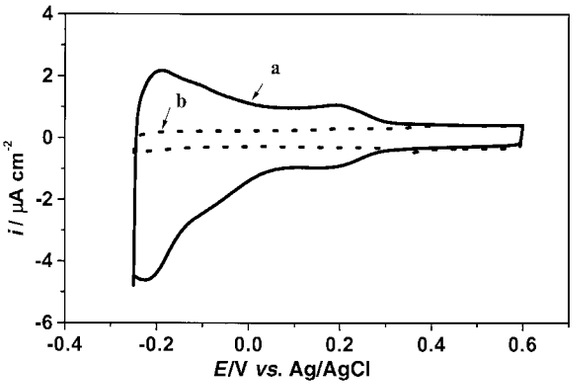

Fig. 1 Cyclic voltammograms of WO_3 deposited for 100 s at (a) 10 μA negative current and (b) pure HOPG in 0.1 mol dm^{-3} H_2SO_4 solution. Scan rate: 50 mV s^{-1}.

comparison. There are no redox signals for HOPG in the same acidic solution, which confirms that WO_3 undoubtedly deposited on the surface of the HOPG.

Fig. 2 shows the surface morphologies of WO_3 deposited at a constant current of 10 μA for different periods of time, recorded using TMAFM. It is observed that isolated nuclei of WO_3 were formed at the first stage of deposition, which then progressively grew to form larger particles (Fig. 2(a)). With increasing deposition time, the neighboring WO_3 particles tended to coalescence to form a linked network (Fig. 2(b)). After monolayer coverage was achieved, WO_3 deposition proceeded continuously and became more uniform (Fig. 2(c) and (d)).

The amount of deposited WO_3 was calculated according to Faraday's law. The average thickness of WO_3 deposited for 10 s is about 2 nm, measured from the AFM image. This datum enables us to calculate the apparent density of deposited WO_3 or the monalayer coverage according to the relative density by comparison with the density of crystalline WO_3. The apparent density is defined as follows:

$$d = \frac{itM}{nFhS_e} \quad (1)$$

where S_e is the apparent surface area of exposed HOPG, M is the molecular weight of tungsten trioxide, h is the mean height (or average thickness) of deposited WO_3, and the other terms have their normal meanings. Electrodeposition is a complex process in the tungsten solution since there are at least three species of undecomposed H_2O_2, polytungstate and peroxy-tungstate in the solution [a more detailed formula for peroxy-tungstate is $[(O)W(O_2)_2(O)(O_2)_2W(O)]^{2-}$ according to reference 12]. It is difficult to determine the value of n in eqn. (1). According to Meulenkamp,[13] a general equation for the decomposition of peroxy-tungstate is given by:

$$W_2O_{11}{}^{2-} + (2+x)H^+ + xe^- = 2WO_3 + (2+x)/2H_2O + (8-x)/4O_2 \quad (2)$$

The variable x in eqn. (2) reflects the complexity of the reduction mechanism and the variability in the extent of reduction due to inhomogeneity of surface morphology, chemical composition, electric potential and the number of possible reductants. When $x=4$, all peroxy groups are completely decomposed and $n=2$ since there are two W atoms involved in eqn. (2). The density of crystalline WO_3 is 7.16 g cm^{-3}. Hence, the apparent densities calculated by eqn. (1) are 0.64, 2.15 and 6.44 g cm^{-3} for WO_3 deposited for 3 s, 10 s and 30 s, respectively. Normally, the porosity of electrodeposited WO_3 is about 50%,[13] therefore 3.58 g cm^{-3} is used as the density of WO_3 formed on HOPG. Based on this assumption, the relative coverages can be obtained: 17.9%, 60.1% and 179.9%, respectively. The latter value of >100% is attributable to the thickness of deposited WO_3 being more than 2 nm, or more than a monolayer.

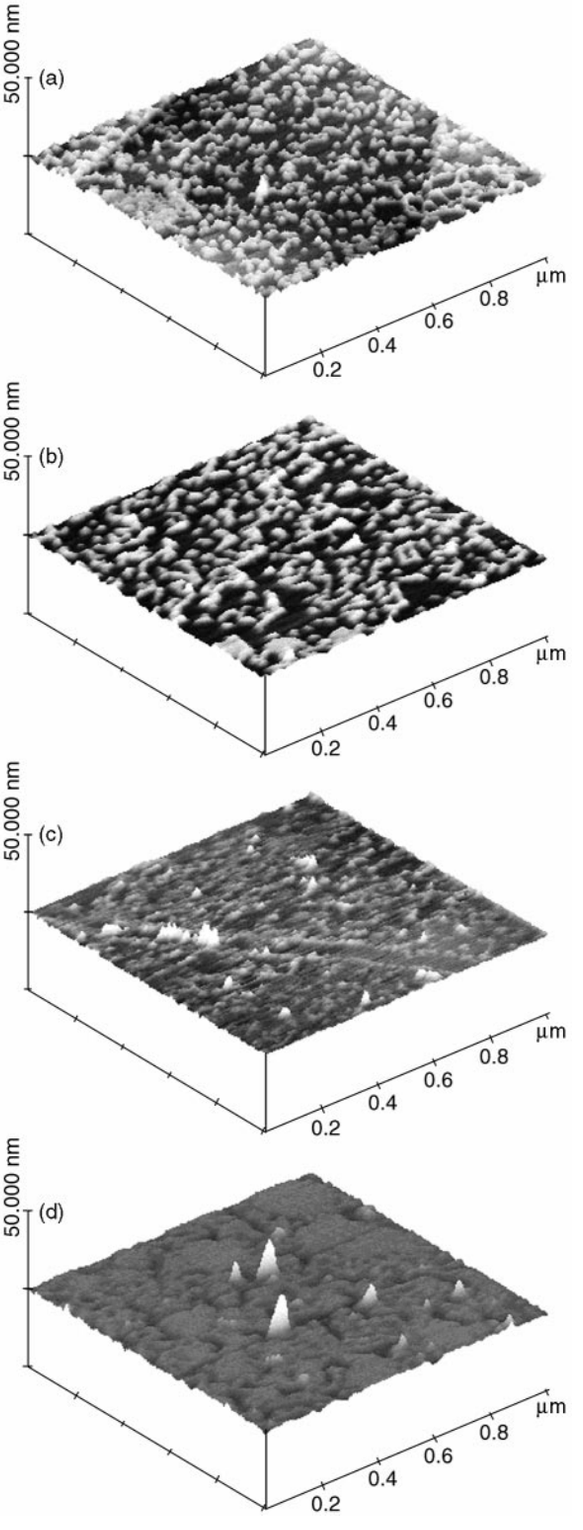

Fig. 2 TMAFM images of WO_3 deposited at 10 μA for (a) 3 s, (b) 10 s, (c) 30 s and (d) 100 s.

There are two features worth noting from the AFM images. First, WO_3 electrodeposited on HOPG is rough with possible internal porosity. By replotting Fig. 2 with an enlarged vertical scale, the roughness can be examined.

The following factors can affect the roughness. (i) The overpotential of WO_3 deposition on HOPG is fairly high. Fig. 3 shows the chronopotentiograms of WO_3 deposition on HOPG at 10 μA. The electrode polarized to about −0.4 V *vs.*

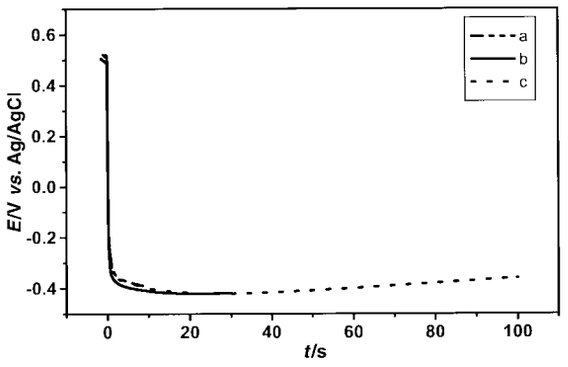

Fig. 3 Chronopotentiograms of WO_3 deposition on HOPG at 10 μA for (a) 10 s, (b) 30 s and (c) 100 s.

Ag/AgCl when a constant current was applied. WO_3 deposition is accompanied by hydrogen evolution at such negative potentials in acidic solution. Therefore, tiny hydrogen bubbles evolved during the WO_3 deposition process may lead to the porosity. (ii) As mentioned above, the electrodeposition of WO_3 is a complex process, however, the main process is the decomposition of peroxy-tungstate on the electrode surface, as described by eqn. (2). When $x=4$, as assumed earlier, there will be free oxygen produced which may or may not be further reduced to water with four more electrons transferred. In addition, the WO_3 produced can receive further electrons by the reversible formation of hydrogen tungsten bronze:[14,15]

$$WO_3 + yH^+ + ye^- \leftrightarrow H_yWO_3 \quad (3)$$

If the oxygen produced cannot be completely reduced to water on the electrode at the same time, oxygen molecules will merge together to form small bubbles. The evolution of oxygen bubbles could be another reason for the formation of a porous WO_3 structure. (iii) The solution used for electrodeposition of WO_3 in this study was an alcohol-containing solution. As shown previously,[8] such a solution composition can greatly improve solution stability and prolong storage time. On the other hand, alcohol molecules have lower surface tension than water and they adsorb preferentially onto the hydrophobic HOPG surface. This leads to the increase in the overpotential for WO_3 deposition. Moreover, the dynamic adsorption and desorption of alcohol molecules interrupts the uniform formation of WO_3 in such an environment. Other results[16] revealed that electrochemically deposited WO_3 in alcohol-containing solution would be more porous.

The second feature worth noting from the AFM images is that with increasing deposition time, the surface roughness changes. According to our AFM investigation, the mean roughness decreased from 0.439 nm to 0.272 nm from Fig. 2(a) to Fig. 2(b). In Fig. 2(c), although the overall roughness increased to 0.354 nm, there are flat regions with local roughness of 0.08 nm. This phenomenon is similar to the leveling process in metal electroplating. The fact that there is a self-leveling effect during the process of WO_3 electrodeposition can be analyzed. As indicated in Fig. 3, the electrode potential dropped to its lowest level at about 20 s and then returned to more positive values at longer times. According to the calculations shown in the earlier paragraph using eqn. (1) and (2), the HOPG surface is already covered by a monolayer of WO_3 after 20 s deposition. This means that WO_3 growth proceeds beyond the monolayer after 20 s at 10 μA in this study. The impediment of hydrogen reduction due to the small overpotential is not only beneficial to WO_3 growth at higher current efficiency, but also reduces surface roughness. Furthermore, the results also show that WO_3 growth occurs more readily on the surface of the initially deposited WO_3 than on the HOPG surface. The electric field distribution should be more uniform on a lower overpotential electrode, leading to more uniform deposits. Hydrogen bubbles were sometimes formed on the surface of the deposited WO_3, but not within the deposits or on the surface of HOPG.

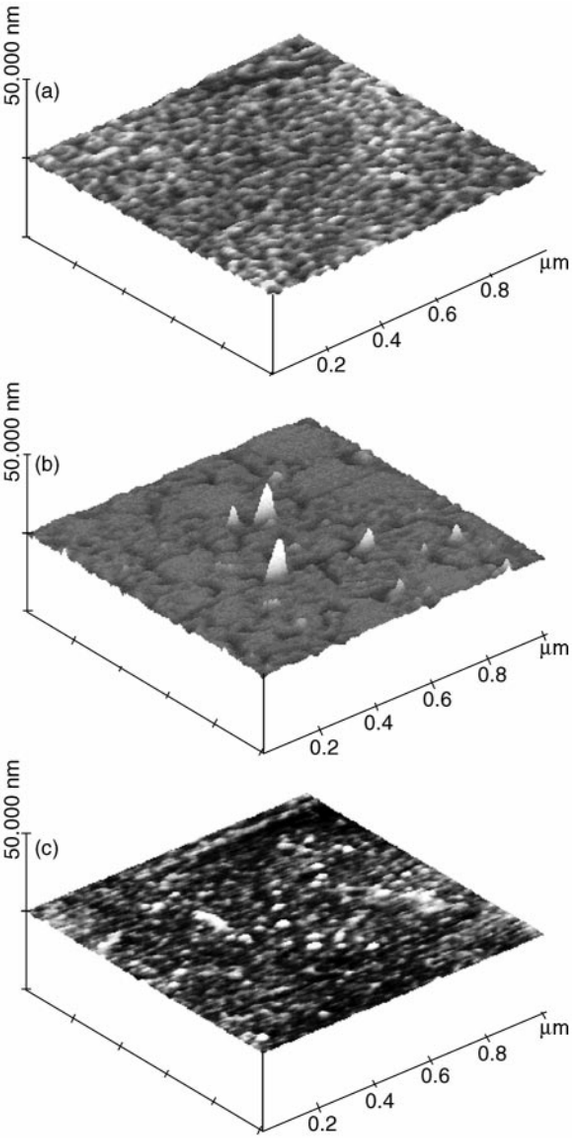

Fig. 4 TMAFM images of WO_3 deposited at (a) 1 μA, (b) 10 μA and (c) 100 μA for a total charge of 1 mC.

The structure and surface morphology of WO_3 are greatly affected by the deposition conditions; this is further exemplified by the following experiments. WO_3 was deposited using the same charge as in the previous experiment, but at various constant currents. Fig. 4 shows the AFM images of WO_3 deposited for a total charge of 1 mC at 1 μA, 10 μA and 100 μA cathodic current, respectively. These images are obviously not alike. At 100 μA only a few, scattered particles were deposited (Fig. 4(c)). The surface of the electrode was well covered but appeared flat when WO_3 was deposited at 1 μA (Fig. 4(a)). As described above, WO_3 deposited at 10 μA was porous (Fig. 4(b)). Cyclic voltammograms of these electrodes in 0.1 mol dm^{-3} H_2SO_4 solution are given in Fig. 5. The characteristic redox peaks of WO_3 are not evident in Fig. 5(a) and (c). The amount of WO_3 deposited is different at different current intensities due to the presence of side reactions. We will analyze the curves in Fig. 6 first (the *x*-axis in Fig. 6 is a logarithmic scale for convenient comparison). Fig. 6(c) is the response curve of WO_3 deposited at 100 μA for 10 s. WO_3 deposition was performed at about −0.8 V and it is obvious that most of the charge was used for hydrogen

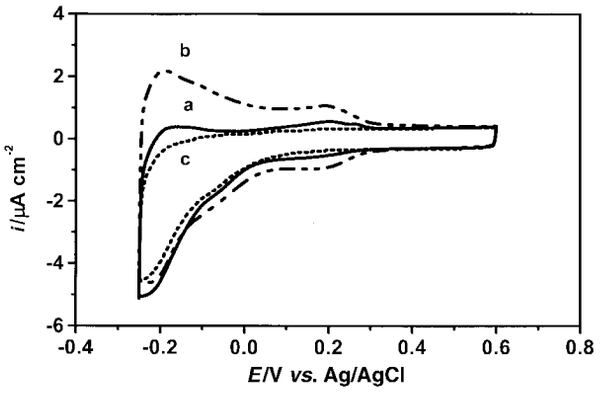

Fig. 5 Cyclic voltammograms of WO_3 deposited at (a) 1 μA, (b) 10 μA and (c) 100 μA for a total charge of 1 mC.

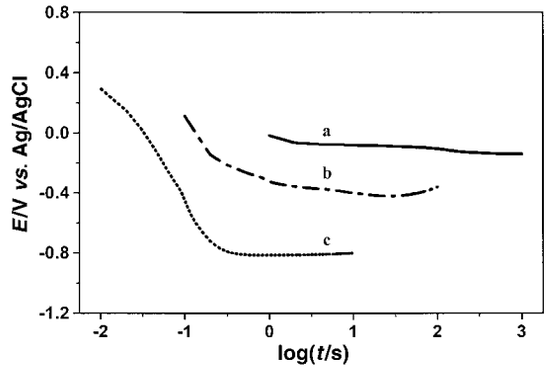

Fig. 6 Chronopotentiograms of WO_3 deposition on HOPG at (a) 1 μA, (b) 10 μA and (c) 100 μA for 1000 s, 100 s and 10 s respectively.

reduction at such a negative potential. Although WO_3 deposition was also favorable at the more negative potential, the deposition time was short and the amount of WO_3 deposited was small due to the lower current efficiency. By contrast, WO_3 was deposited at a less negative potential (−0.1 V *vs.* Ag/AgCl) at 1 μA. It is likely that almost all of the charge was used for WO_3 deposition (see Fig. 6(a)). The deposition was very slow and without the interference of hydrogen evolution. The electric field distribution was quite uniform under a small current and, hence, the deposited WO_3 was uniform and dense. Dense WO_3 means a low real surface area which affects the coloration efficiency and response time, since electrochemical reactions take place at the interface between the electrode and the electrolyte. We now return to Fig. 4 and Fig. 5. The AFM images in Fig. 4 are in fairly good agreement with the explanation. In the cases of larger and lower deposition current shown above, their electrochromic behavior reflected in the cyclic voltammograms is small (Fig. 5(a) and (c)). Though the amount of WO_3 deposited at 1 μA is more than that deposited at 10 μA, the electrochromic behavior is not as good as that deposited at 10 μA. A fair electrochromic WO_3 deposit can be prepared only under suitable conditions. The results indicate that the electrochromic properties of WO_3 depend not only on the amount deposited but also on the structure and morphology of the deposit.

Conclusions

Electrodeposition is a convenient and useful method for preparing electrochromic WO_3 even on the hydrophobic surface of highly oriented pyrolytic graphite (HOPG). The deposited WO_3 was porous and had a rough surface. Tapping mode atomic force microscopic (TMAFM) observation revealed that the growth of electrodeposited WO_3 on HOPG can be described as a nucleation–coalescence mechanism in the early stages, and the growth sequence has four stages: (1) formation of isolated nuclei and their growth to larger grains, (2) coalescence of larger grains, (3) formation of a linked network, and (4) formation of a continuous deposit. This sequence of growth stages is clearly illustrated in Fig. 2.

Since the overpotential of WO_3 deposition on previously deposited WO_3 is lower than that on bare HOPG, the roughness tends to decrease after monolayer coverage of the HOPG surface by WO_3 at longer times under constant current, showing a self-leveling process.

Acknowledgements

Supports from the Conference and Research Grants Committee of the University of Hong Kong and the Research Grants Council of Hong Kong (HKU 7089/98P) are acknowledged.

References

1 S. K. Deb, *Appl. Opt. Suppl.*, 1969, **3**, 193.
2 P. M. S. Monk, R. J. Mortimer and D. R. Rosseinsky, *Electrochromism: fundamentals and applications*, VCH, Weinheim, 1995.
3 C. G. Granqvist, *Electrochim. Acta*, 1999, **44**, 3005.
4 R. D. Rauh, *Electrochim. Acta*, 1999, **44**, 3165.
5 P. K. Shen and A. C. C. Tseung, *J. Mater. Chem.*, 1992, **2**, 1141.
6 P. K. Shen, K. Y. Chen and A. C. C. Tseung, *J. Electrochem. Soc.*, 1994, **141**, 1758.
7 X. G. Wang, Y. S. Jiang, N. H. Yang, L. Yuan and S. J. Pang, *Appl. Surf. Sci.*, 1999, **143**, 135.
8 K. J. Stevenson, G. J. Hurtt and J. T. Hupp, *Electrochem. Solid-State Lett.*, 1999, **2**, 175.
9 P. K. Shen and A. C. C. Tseung, *J. Electrochem. Soc.*, 1994, **141**, 3082.
10 A. C. C. Tseung, P. K. Shen and K. Y. Chen, *J. Power Sources*, 1996, **61**, 223.
11 P. K. Shen, J. Syed-Bokhari and A. C. C. Tseung, *J. Electrochem. Soc.*, 1991, **38**, 2778.
12 K. Yamanaka, *Jpn. J. Appl. Phys.*, 1987, **26**, 1884.
13 E. A. Meulenkamp, *J. Electrochem. Soc.*, 1997, **144**, 1664.
14 B. Reichman and A. J. Bard, *J. Electrochem. Soc.*, 1979, **126**, 583; 2133; 1980, **127**, 647.
15 P. J. Kuleza and L. R. Faulkner, *J. Electroanal. Chem.*, 1988, **248**, 305.
16 P. K. Shen, K. Y. Chen and A. C. C. Tseung, *Proceedings of the Symposium on Electrochromic Materials II*, The Electrochemical Society, Pennington, NJ, 1994, vol. 94, p. 14.

Paper a908348k